Electron effective mass and nonparabolicity in $Ga_{0.47}In_{0.53}As/InP$ quantum wells

C. Wetzel*
Physik-Department E16, Technische Universität München, James-Franck-Strasse, 85747 Garching, Germany

R. Winkler†
Institut für Theoretische Physik, Universität Regensburg, 93040 Regensburg, Germany

M. Drechsler and B. K. Meyer
Physik-Department E16, Technische Universität München, James-Franck-Strasse, 85747 Garching, Germany

U. Rössler
Institut für Theoretische Physik, Universität Regensburg, 93040 Regensburg, Germany

J. Scriba and J. P. Kotthaus
Sektion Physik, Ludwigs-Maximilians-Universität München, Geschwister-Scholl-Platz, 80539 München, Germany

V. Härle and F. Scholz
Physikalisches Institut, Universität Stuttgart, Pfaffenwaldring 57, 70569 Stuttgart, Germany
(Received 11 September 1995)

The in-plane effective electron mass ($m_\parallel$) in narrow $Ga_{0.47}In_{0.53}As/InP$ quantum wells is strongly dependent on the quantization energy. Cyclotron resonance in a series of quantum wells with well widths down to 15 Å reveals a mass enhancement of up to 50% ($m_\parallel = 0.065 m_0$) over the bulk value of $Ga_{0.47}In_{0.53}As$. This effect is caused by the nonparabolicity of the conduction band and wave function penetration into the barrier material. Our experimental findings are in good agreement with calculations performed within the framework of $\mathbf{k}\cdot\mathbf{p}$ theory. We obtain an easy-to-use relation between the mass and the quantization energy $m_0/m_\parallel(\epsilon) = (1 - 1.96\epsilon/\mathrm{eV})/0.044$.

Considerable progress in epitaxial growth techniques has led to high-quality quantum well (QW) structures with a ternary well material. State-of-the-art heterostructure devices like QW lasers and high electron mobility transistors make use of very narrow QW's in $Ga_xIn_{1-x}As/InP$ and $Ga_xIn_{1-x}As/GaAs$ systems.[1] Simulation and design of these devices rely on an accurate determination of the basic band-structure parameters such as the effective electron mass responsible for the optical properties and in-plane transport.

The effect of forming a QW is twofold: (i) The continuum of bulk band states splits into subbands whose quantization energies increase as the well width decreases. (ii) Free motion of electrons is possible only in the plane of the QW. For small quantization energies and small kinetic energies of the electrons compared to the fundamental gap the subband energies and the subband dispersion can be described by the effective mass of the bulk conduction band edge. For narrow QW's and narrow-gap materials, however, deviations from this parabolic model become important, which can be described by an energy-dependent effective mass $m^*(\epsilon)$. The axial symmetry of the QW allows for different masses for the motion in the plane of the QW, $m_\parallel(\epsilon)$, and perpendicular to it, $m_\perp(\epsilon)$.[2] Due to its larger fundamental gap the barrier material has a larger band-edge mass than the well material. Therefore, in narrow QW's with quantization energies comparable to the band offset, penetration of the subband wave function into the barrier material becomes increasingly important.

Unlike the well-studied $GaAs/Al_xGa_{1-x}As$ QW's, little is known about the band-structure effects in $Ga_{0.47}In_{0.53}As/InP$ QW's. In this work we present cyclotron resonance (CR) data of the in-plane effective electron mass $m_\parallel$ in $Ga_{0.47}In_{0.53}As/InP$ QW's for a wide range of well widths down to only a few monolayers. In an earlier paper our experiments were limited to rather wide wells[3] but with improved mobilities the narrow wells became accessible, which are relevant in state-of-the-art heterostructure devices. Conventional CR is obtained on doped samples while optically detected CR (ODCR) allows us to study also undoped samples;[4,5] i.e., we determine $m_\parallel$ directly at the bottom of the subband and filling effects can be neglected. A substantial increase of $m_\parallel$ is observed for decreasing well width. The experimental data are compared with calculations based on two $\mathbf{k}\cdot\mathbf{p}$ models of different refinement. An analytical expression is given to relate $m_\parallel$ to the electron quantization energy, which can be derived from optical experiments.

The $Ga_{0.47}In_{0.53}As/InP$ samples were grown by low-pressure metal-organic chemical vapor deposition.[6] The well widths vary from $L_z = 200$ Å down to 15 Å. Part of the samples are n-type modulation doped. As a bulk reference, a 1-μm $Ga_{0.47}In_{0.53}As$ epitaxial layer on InP is investigated. Photoluminescence (PL) was excited with a 632.8-nm HeNe laser (5 mW) or a 514.5-nm Ar^+ laser (20 mW) through a single optic fiber that also guided the luminescence light. By its wider divergence the luminescence light was separated from the laser beam, dispersed by a 0.25-m monochromator,

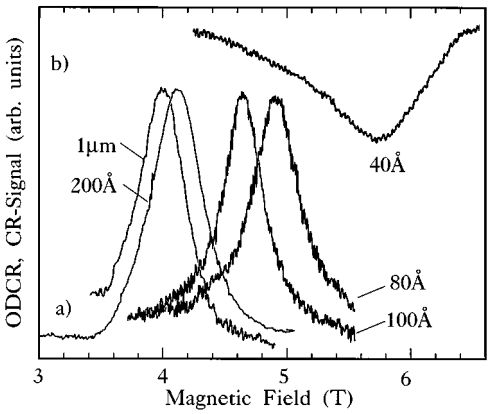

FIG. 1. (a) ODCR (shown as a positive signal) and (b) conventional CR of QW's with different layer thicknesses. The $Ga_{0.47}In_{0.53}As$ bulk signal (1 μm) is given for reference.

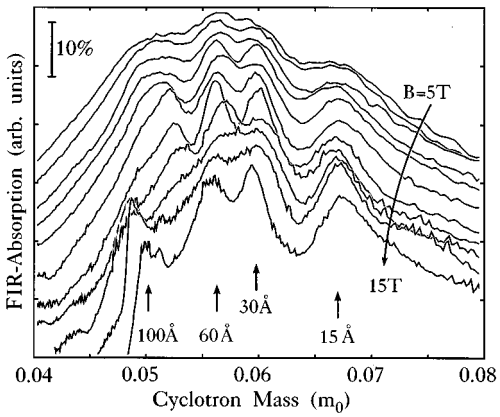

FIG. 2. CR absorption (shown as a positive signal) of a MSQW sample containing QW's with $L_z = 15$, 30, 60, and 100 Å detected by FTIR spectrometry in the range of $1/\lambda = 80$–$300\ \mathrm{cm}^{-1}$. The abscissa is rescaled to the cyclotron mass $m_c = eB\lambda/2\pi c$.

and detected by a Ge detector (North Coast). CR was excited in the far-infrared (FIR) at $\lambda_{FIR} = 118\ \mu$m using a gas laser system (Edinburgh Instruments). The FIR radiation was modulated by means of a mechanical chopper at 27 Hz, which allowed for lock-in detection of the resonant changes in the PL. In addition, a Fourier transform infrared (FTIR) spectrometer (Bruker) in combination with a Ge bolometer was used. Superconducting magnets provided fields up to 15 T.

Typical ODCR signals are shown in Fig. 1(a) for QW's with well width $L_z = 200$ Å (nominally undoped), 100 Å, and 80 Å. The latter two samples are n-type doped with carrier concentrations $N_n = 5.8\times10^{11}$ and $6.0\times10^{11}\ \mathrm{cm}^{-2}$, respectively. For comparison we also show the spectrum of a 1-μm epitaxial $Ga_{0.47}In_{0.53}As$ layer. PL was detected at the recombination energy of the bound exciton and the intensity is monitored with respect to the modulated FIR radiation. When sweeping the magnetic field we observe a strong decrease of the PL intensity (shown as a positive signal here). The ODCR signal observed is up to 5% of the PL intensity. A detailed study of the coupling mechanisms has been given elsewhere.[7] Due to the sensitivity of the ODCR method the small number of photogenerated carriers in the undoped samples is sufficient to observe these signals.

With decreasing well width the position of the resonances strongly shifts towards higher magnetic field. Values for the cyclotron mass m_c are derived using the relation $m_c = eB_{res}\lambda/2\pi c$ with c the speed of light (Système International units). In the undoped samples m_c is determined directly at the bottom of the subband whereas in the doped samples, m_c is obtained at the Fermi energy.

Additional results are obtained by conventional CR for a well with $L_z = 40$ Å and $N_n = 5.9\times10^{11}\ \mathrm{cm}^{-2}$. In transmission geometry under conditions identical to the ODCR experiment the resonance is observed at an even higher field position [Fig. 1(b)], shifting from $B = 4$ T in the bulk material to up to 5.7 T in the 40-Å well. This shift is accompanied by an increase of the resonance line width, which can be attributed to higher scattering rates in the narrow wells.[8,9]

A whole set of mass values is derived from a sample containing several QW's each grown under identical conditions. This multiple single quantum well (MSQW) structure contains wells with $L_z = 100,\ 60,\ 30$, and 15 Å with a doping layer symmetrically adjacent to each well separated by a spacer (50 Å). Conventional CR data were taken by a FTIR spectrometer and the absorption is displayed in Fig. 2. The FIR spectra are taken in the range of wave numbers $1/\lambda = 80 - 300\ \mathrm{cm}^{-1}$ and the magnetic field was stepped from $B = 5$ T to 15 T with $\Delta B = 1$ T. For ease of interpretation the abscissa is rescaled to $m_c = eB\lambda/2\pi c$. In each trace several resonances are observed, which stem from the 100-, 60-, 30-, and 15-Å wells. To our knowledge the 15-Å-wide QW studied here is the narrowest ternary QW to show CR. With increasing field the resonances are resolved better as the wave function shrinks. In the high-field region, distortion of the line shapes and jumps towards lower masses are observed for the two broader wells (100 and 60 Å). Such an effect is known to coincide with the depopulation of a Landau level. We thus estimate a carrier concentration $N_n \approx 6\times10^{11}\ \mathrm{cm}^{-2}$ for these two wells. Although every well has an adjacent doping layer, no filling effects can be observed in the narrow wells. This can result from the high quantization energy and the band bending along the spacer between dopants and well. These findings are further supported by PL experiments where no Fermi edge is observable on a logarithmic scale.[10] To derive effective mass values $m_\parallel$ the peak positions are linearly extrapolated to zero magnetic field.

All values of $m_\parallel$ are collected in Fig. 3 and plotted versus the QW thickness. For zero well width the experimental value for bulk InP $m_0^* = 0.080 m_0$ is also shown.[4] The increase of $m_\parallel$ compared to the bulk value $m_0^* = 0.044 m_0$ is dramatic. The highest observed mass is $m_\parallel = 0.065 m_0$ in the 15 Å well, which corresponds to an increase by almost 50 %. Such a strong variation of $m_\parallel$ is of high relevance for the interpretation of optical and transport experiments and device design. A similar strong mass enhancement has been observed by Hendorfer *et al.*[11] in an asymmetric 20-Å $Ga_{0.8}In_{0.2}As$ QW cladded by $Al_{0.3}Ga_{0.7}As$ and GaAs. Shubnikov–de Haas results by Wiesner [12] and Schneider [13] are included in Fig. 3.

In order to analyze the contributions of nonparabolicity and penetration into the barrier we performed two calcula-

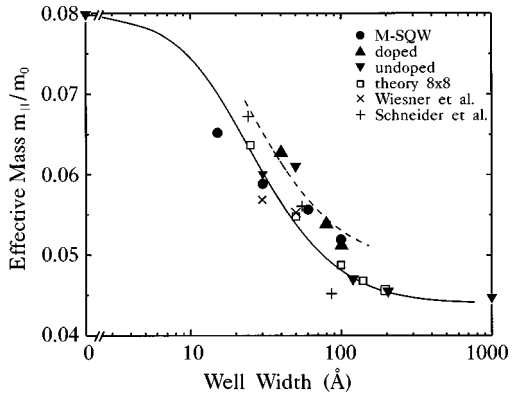

FIG. 3. The in-plane effective mass as a function of the well width. Experimental values for undoped and doped samples are given. Calculated results are indicated by a full line ($N_n=0$), dashed line ($N_n=6\times10^{11}\ \mathrm{cm}^{-2}$), both obtained with the modified Kane formula, and open squares (8×8 Hamiltonian). Experimental data from Wiesner *et al.* (Ref. 12) and Schneider *et al.* (Ref. 13) is also included (for error bars see original work).

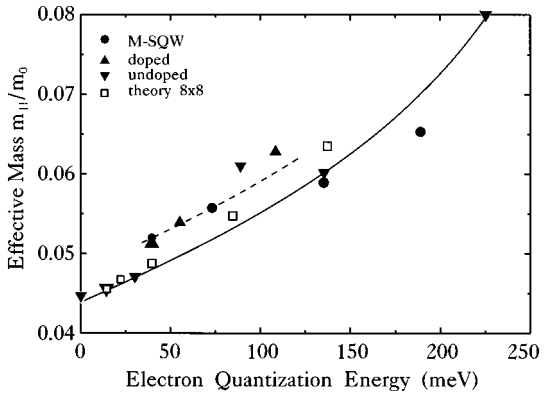

FIG. 4. The in-plane effective mass as a function of the calculated electron quantization energy. Symbols and lines correspond to Fig. 3.

tions within the framework of $\mathbf{k}\cdot\mathbf{p}$ theory for zero magnetic field. In the first approach we use the model of a square well with finite barriers but with an energy-dependent effective mass characterized by a modified Kane formula[14,15]

$$\frac{m_0}{m^*(\epsilon)}=1+2F+\frac{2m_0P^2}{3\hbar^2}\left(\frac{2}{E_g+\epsilon}+\frac{1}{E_g+\Delta+\epsilon}\right). \quad (1)$$

Here ϵ is the confinement energy of the lowest subband, P is Kane's momentum matrix element, and F accounts for coupling to remote bands.[16] Flux conserving boundary conditions for the envelope function ϕ are used, i.e., we assume continuity of ϕ and $(1/m^*)d\phi/dz$.

The effective mass $m_{\|}(\epsilon)$ for the in-plane motion can be defined via the second derivative of the subband dispersion $\epsilon_n(k_{\|})$. In a CR experiment, however, a finite perturbation is applied by the magnetic and the dispersion is averaged over the Landau level splitting equivalent to a finite $\delta k_{\|}$. The curvature of the band is thus experienced as the slope between the initial and final state. The effective mass is then given by

$$\frac{1}{m_{\|}(\epsilon)}=\frac{1}{\hbar^2k_{\|}}\frac{\delta\epsilon}{\delta k_{\|}}. \quad (2)$$

This mass is frequently called the density-of-states effective mass[17] or the momentum effective mass. In the limit $B\to0$ the cyclotron mass m_c equals $m_{\|}(\epsilon)$ evaluated at the Fermi edge $\epsilon=\epsilon_F$ [the subband edge $\epsilon=\epsilon_n(k_{\|}=0)$ in undoped samples]. We thus compare measured cyclotron masses with theoretical values for $m_{\|}(\epsilon)$ calculated by means of Eq. (2). We note that Eq. (2) is the relevant definition of an effective mass for an interpretation of most optical and transport related experiments.

In the second approach we use an 8×8 $\mathbf{k}\cdot\mathbf{p}$ Hamiltonian,[18] which explicitly takes into account the off-diagonal $\mathbf{k}\cdot\mathbf{p}$ coupling between the lowest conduction band Γ_6^c, the topmost valence band Γ_8^v, and the split-off valence band Γ_7^v as well as remote band contributions of second order in $\mathbf{k}$. In momentum space the multicomponent envelope function problem becomes a set of coupled integral equations, which we solve numerically by means of a quadrature method.[17] In this way we obtain subband dispersion curves $\epsilon_n(\mathbf{k}_{\|})$, which fully take into account nonparabolicity. Here we are interested only in the lowest subband $n=0$. By means of an analytic quadratic Brillouin zone integration scheme[19] we then calculate from $\epsilon_0(\mathbf{k}_{\|})$ the density-of-states effective mass $m_{\|}(\epsilon)$. Band parameters are taken from Ref. 20. However, according to our experimental findings the effective mass $m_0^*=0.044m_0$ is used for $Ga_{0.47}In_{0.53}As$.[21]

Figure 3 shows $m_{\|}$ at the bottom of the lowest subband as a function of the well width L_z. The results of the first approach are given by the solid line. The second calculation yields the values indicated by open squares. Starting from the bulk value of $Ga_{0.47}In_{0.53}As$, $m_{\|}$ strongly increases with decreasing L_z and smoothly approaches the InP bulk band edge mass $m^*=0.080m_0$ for vanishing well width. For the doped samples an additional mass enhancement is taken into account by considering the effective mass at the Fermi energy. The dashed line in Fig. 3 corresponds to $N_n=6\times10^{11}\ \mathrm{cm}^{-2}$. Both calculations give very similar results in the overlapping range from 25 to 200 Å. They explain the experimental findings of $m_{\|}$ very well.

The variation of $m_{\|}$ can be most clearly related to the band structure by plotting $m_{\|}$ versus the energy of the subband edge $\epsilon_0(k_{\|}=0)$ (Fig. 4). Note that both models predict slightly different energies for the same well width. Our results (solid line in Fig. 4) can be parametrized by

$$\frac{m_0}{m_{\|}(\epsilon)}=\frac{m_0}{m_0^*}(1-\eta\epsilon)=\frac{1}{0.044}\left(1-1.96(4)\frac{\epsilon}{\mathrm{eV}}\right). \quad (3)$$

We note that one has to distinguish the dependence of $m_{\|}$ on the subband quantization energy given in Eq. (3) from the energy dependence of $m_{\|}$ due to the in-plane motion. For a fixed well width and each subband n the effective mass $m_{\|}$ is known to depend linearly on ϵ (Refs. 17 and 22) while in Eq. (3) $1/m_{\|}$ depends linearly on ϵ. The reason for the different functional dependences is that in the former case the probability ratio for finding the electrons in the well and in the barriers is basically independent of ϵ (i.e., independent of

$k_\parallel$) whereas this ratio varies with well width so that the subband states are affected by the larger effective mass in the barriers. This effect is in particular important due to the comparatively small conduction-band offset $\Delta E_c = 224$ meV in $Ga_{0.47}In_{0.53}As$/InP QW's.[3] For the same reason one cannot compare our results with nonparabolicity parameters η, which have been derived by analyzing intersubband transitions in *one* QW (Refs. 23 and 24) or those reported for bulk $Ga_{0.47}In_{0.53}As$.[25]

Equation (3) gives a good approximation to our calculation within the whole energy range $0 \leqslant \epsilon \leqslant \Delta E_c$. A similar expression was found from magnetoluminescence on a doped 100-Å QW with a parameter $\eta = 2.9(5)\ \mathrm{eV}^{-1}$.[23] It is also a reasonable approximation to the theoretical analysis in Ref. 26.

Equation (3) can be used to determine the effective mass directly from the optical properties of the structure. In an experiment the energy ϵ is approximately given by the PL energy of the electron–heavy-hole transition minus the bulk band gap. Due to the light electron mass the electron quantization energy accounts for about 90% of the observed energy shift whereas the quantization energy of the heavy-hole states ($\epsilon \leqslant 42$ meV at $L_z \geqslant 40$ Å) can be neglected.

In summary, we determined by CR the in-plane effective electron mass $m_\parallel$ in $Ga_{0.47}In_{0.53}As$/InP QW's for a wide range of well widths. We experimentally observe a very large enhancement of about 50% in a 15-Å QW. The observation of CR in such a narrow ternary QW is especially worth mentioning. The dependence of $m_\parallel$ on the quantization energy can be parametrized by Eq. (3). The effective mass $m_\parallel$ is responsible for electron transport and optical properties. Therefore these results can be of great importance for simulation, design, and characterization of heterostructures and devices based on $Ga_{0.47}In_{0.53}As$/InP.

*Present address: Lawrence Berkeley National Laboratory, University of California, Berkeley, CA 94720.

†Present address: Department of Physics and Astronomy, Vanderbilt University, Nashville, TN 37235.

[1] H. Sakaki, Solid State Commun. **92**, 119 (1994).

[2] U. Ekenberg, Phys. Rev. B **40**, 7714 (1989).

[3] C. Wetzel, Al. L. Efros, B. K. Meyer, A. Moll, P. Omling, and P. Sobkowicz, Phys. Rev. B **45**, 14 052 (1992).

[4] A. Moll, C. Wetzel, B. K. Meyer, P. Omling, and F. Scholz, Phys. Rev. B **45**, 1504 (1992).

[5] C. Wetzel, B. K. Meyer, and P. Omling, Phys. Rev. B **47**, 15 588 (1993).

[6] K. Streubel, V. Härle, F. Scholz, M. Bode, and M. Grundmann, J. Appl. Phys. **71**, 3300 (1992); V. Härle, Ph.D. thesis, University Stuttgart, 1995.

[7] D. M. Hofmann, M. Drechsler, C. Wetzel, B. K. Meyer, F. Hirler, R. Strenz, G. Abstreiter, G. Böhm, and G. Weimann, Phys. Rev. B **52**, 11 313 (1995).

[8] U. Bockelmann, G. Abstreiter, G. Weimann, and W. Schlapp, Phys. Rev. B **41**, 7864 (1990).

[9] A. Gold, Phys. Rev. B **38**, 10 798 (1988).

[10] R. Küchler, G. Abstreiter, G. Böhm, and G. Weimann, Semicond. Sci. Technol. **8**, 88 (1993).

[11] G. Hendorfer, M. Seto, H. Ruckser, W. Jantsch, M. Helm, G. Brunthaler, W. Jost, H. Obloh, K. Köhler, and D. J. As, Phys. Rev. B **48**, 2328 (1993).

[12] U. Wiesner, J. Pillath, W. Bauhofer, A. Kohl, A. Mesquida Küsters, S. Brittner, and K. Heime, Appl. Phys. Lett. **64**, 2520 (1994).

[13] D. Schneider, L. Elbrecht, J. Creutzburg, A. Schlachetzki, and G. Zwinge, J. Appl. Phys. **77**, 2828 (1995).

[14] E. O. Kane, J. Phys. Chem. Solids **1**, 249 (1957).

[15] For $Ga_{0.47}In_{0.53}As$ we may consider an 8×8 $\mathbf{k}\cdot\mathbf{p}$ Hamiltonian (Γ_6^c, Γ_8^v, and Γ_7^v) that neglects remote band contributions and the free electron term. If we restrict ourselves to $\mathbf{k}_\parallel = 0$ then the envelope function problem consists of a set of coupled first-order differential equations, which can be transformed into two second-order differential equations for the conduction-band envelope functions. These equations have the usual form of a one-dimensional Schrödinger equation with an effective mass given by the third term of Eq. (1).

[16] P. Sobkowicz, Semicond. Sci. Technol. **5**, 183 (1990).

[17] R. Winkler and U. Rössler, Phys. Rev. B **48**, 8918 (1993).

[18] H.-R. Trebin, U. Rössler, and R. Ranvaud, Phys. Rev. B **20**, 686 (1979).

[19] R. Winkler, J. Phys.: Condens. Matter **5**, 2321 (1993).

[20] *Semiconductors, Physics of Group IV Elements and III-V Compounds*, edited by H. Hellwege and O. Madelung, Landolt-Börnstein, New Series, Group III, Vol. 17, Pt. a (Springer, Berlin, 1982); *Semiconductors, Intrinsic Properties of Group IV Elements and III-V, II-VI and I-VII Compounds*, edited by H. Hellwege and O. Madelung, Landolt-Börnstein, New Series, Group III, Vol. 22, Pt. a (Springer, Berlin, 1987).

[21] Although in $Ga_{0.47}In_{0.53}As$ the observation of $m_0^* = 0.044 m_0$ differs from commonly cited values (Ref. 20) similar values have been obtained by M. S. Skolnick *et al.* [Solid State Commun. **67**, 637 (1988)], D. G. Hayes *et al.* [Surf. Sci. **229**, 512 (1990)], and P. E. Simmonds *et al.* [Solid State Commun, **67**, 1151 (1988)]. It is also within the error bars of experimental data published by R. J. Nicholas *et al.* [Appl. Phys. Lett. **34**, 492 (1979)].

[22] For a 100-Å-wide $Ga_{0.47}In_{0.53}As$/InP QW and $\epsilon \leqslant 400$ meV our calculations based on the second approach yield $m_\parallel(\epsilon)/m_0 = 0.045(1 + 2.62\epsilon/\ \mathrm{eV})$ for the lowest electron subband and $m_\parallel(\epsilon)/m_0 = 0.046(1 + 2.62\epsilon/\ \mathrm{eV})$ for the first excited subband.

[23] D. J. Mowbray, J. Singleton, M. S. Skolnick, N. J. Pulsford, S. J. Bass, L. L. Taylor, R. J. Nicholas, and W. Hayes, Superlatt. Microstruct. **3**, 471 (1987).

[24] J. Oikine-Schlesinger, E. Ehrenfreund, D. Gershoni D. Ritter, M. B. Panish, and R. A. Hamm, Appl. Phys. Lett. **59**, 970 (1991).

[25] D. Gershoni and H. Temkin, J. Lumin. **44**, 381 (1989).

[26] B. R. Nag and S. Mukhopadhyay, Appl. Phys. Lett. **62**, 2416 (1993).